ISSN 1063-7842, Technical Physics, 2019, Vol. 64, No. 6, pp. 859–863. © Pleiades Publishing, Ltd., 2019.
Russian Text © The Author(s), 2019, published in Zhurnal Tekhnicheskoi Fiziki, 2019, Vol. 89, No. 6, pp. 913–917.

PHYSICAL SCIENCE OF MATERIALS

Substructure of Intermetallic Thin-Film Cu_3Sn

A. N. Mokrushina[a], V. A. Plotnikov[a,*], B. F. Dem'yanov[a], and S. V. Makarov[a]

[a] *Altai State University, Barnaul, 656049 Russia*

**e-mail: plotnikov@phys.asu.ru*

Received August 1, 2018; revised August 1, 2018; accepted December 1, 2018

Abstract—The crystalline structure of intermetallic Cu_3Sn synthesized by successively condensing thin layers of copper and tin on a substrate at 150°C has been studied. Cu_3Sn compound exists in a very narrow homogeneity range and has a long-period close-packed ordered $D0_{19}$ superstructure. It has been found that the crystal lattice exhibits many slip traces associated with dislocation motion. The dislocation motion is due to the stressed state of the crystal, which can be characterized as uniform extension. Electron micrographs show that slip traces in the Cu_3Sn crystal are parallel to the $(\bar{1}\bar{1}21)$ and $(11\bar{2}1)$ planes belonging to pyramidal slip system II, which is a main slip system along with pyramidal and basal ones. Slip traces result from the motion of partial dislocations, as indicated by the amount of slip, which is equal to half the interplanar distance. Since the crystal is ordered, slip is accomplished by a pair of superpartial dislocations and a slip trace may be a superstructural or complex stacking fault.

DOI: 10.1134/S1063784219060112

INTRODUCTION

In recent years, the structure and properties of Cu_3Sn intermetallic have attracted much attention from researchers engaged in various fields of condensed matter physics. Cu_3Sn and Cu_6Sn_5 intermetallics are the only two phases from the Cu–Sn system existing at room temperature. The properties of Cu_3Sn and Cu_6Sn_5 intermetallics are of great importance for microelectronics because of their uncontrolled formation at the tin–copper interface. This generates local stresses and results in cracking, which adversely affects the strength of soldered contacts [1, 2]. Usually, contact damage takes place along an intermetallic layer [3, 4], although a thin intermetallic phase may exert a beneficial effect, improving the adhesive strength of solder–substrate interfaces [5–7].

In spite of the fact that the Cu_3Sn phase exists in all systems containing a Cu–Sn contact, it can be used as an independent material to synthesize coatings and thin films [8, 9]. The crystal structure of Cu_3Sn persists up to the melting point, thereby allowing bulk single crystals of this compound to be grown by the standard Bridgman method. Therefore, research on the strength and deformation properties of Cu_3Sn crystals has become of great significance.

Stoichiometric Cu_3Sn compound has a $D0_{10}$ superstructure [10], which can be represented as a stack of identical hexagonal layers ....abababab.... . The $D0_{19}$ superstructure is similar to $L1_2$, in which hexagonal layers alternate in sequence .... abcabcabcabc.... . The $D0_{19}$ superstructure is typical of many metals and metallic compounds, such as Mg, Cd, Cd_3Mg, Cu_3Ti, Ti_3Sn, Mn_3Sn, and Ti_3Al. Most studies were devoted to Ti_3Al intermetallic. As for Cu_3Sn, its properties remain obscure. It is known that many crystals with an $L1_2$ superstructure exhibit an anomalous temperature dependence of strength characteristics [11]. Similar temperature anomalies may also be expected in intermetallics with a $D0_{19}$ superstructure.

Single crystals with a $D0_{19}$ superstructure (hereinafter, $D0_{19}$ crystals or compounds) are difficult to study, because temperature anomalies in them combine with the orientation dependence of deformation. In $D0_{19}$ compounds, yield stress strongly depends on the direction of deformation. For example, for deformation in the [0001] direction in Ti_3Sn, yield stress at room temperature equals 200 MPa and decreases with growing temperature (normal behavior). However, when the orientation differs by 40°, yield stress rises to 1200 MPa and continues rising with temperature (anomalous behavior) [12]. The sharp orientation dependence of mechanical properties and the low ductility of $D0_{19}$ alloys at room temperature are explained by a small amount of slip systems that facilitate deformation for the given direction of loading [12]. To shed light on the behavior of $D0_{19}$ alloys, it is necessary to perform direct investigation of dislocation slip systems to find active slip planes and slip directions, determine the Burgers vectors of superdislocations, and see how superdislocations split into

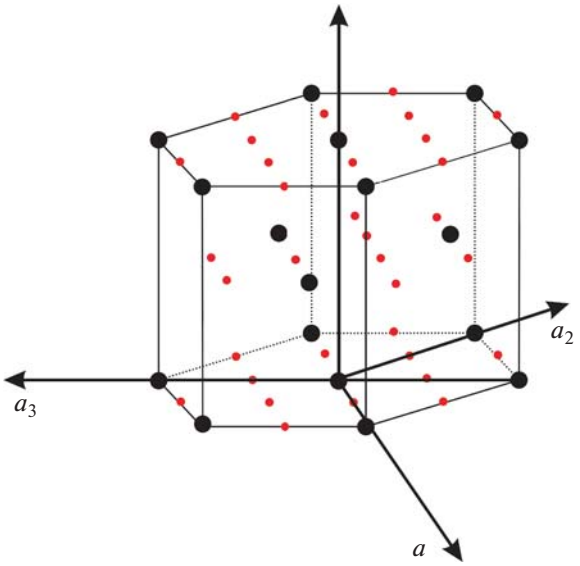

Fig. 1. Unit cell of the $D0_{19}$ superstructure. Grey and black dots stand for copper and tin atoms, respectively.

partial dislocations with the formation of surface defects (twin boundaries, stacking faults).

Here, we study the structure of intermetallic Cu_3Sn, which is synthesized in Cu/Sn binary films along with intermetallic Cu_6Sn_5.

MATERIAL AND STRUCTURE EXAMINATION

To study the structure and formation mechanism of intermetallics Cu_3Sn and Cu_6Sn_5, we successively applied two layers of pure metals on a glass substrate (first Cu and then Sn) by thermal evaporation in vacuum. During condensation of Cu/Sn layers, the substrate was kept at 150°C.

Structural examination was carried out in the IRGETAS laboratory at the Serikbaev East Kazakhstan State Technical University under a JEM-2100 scanning electron microscope at an accelerating voltage of 200 kV.

CRYSTAL STRUCTURE

At the early stage of investigation, the crystal structure of intermetallic Cu_3Sn was assigned to the orthorhombic system [13] with lattice parameters a = 0.549 nm, b = 0.432 nm, and c = 0.474 nm [14].

Cu_3Sn compound, as well as many other intermetallics, exists in a very narrow homogeneity range and has an ordered $D0_{19}$ superstructure [15, 16]. Its stoichiometric formula can be written as AB_3. The crystal lattice of $D0_{19}$ alloys can be represented as a stack of identical hexagonal atomic layers. Each layer consists of A and B atoms in a stoichiometric ratio. The sequence of layers in the $D0_{19}$ superstructure is the same as in the lattice of hcp metals. The unit cell of the $D0_{19}$ superstructure is shown in Fig. 1.

Subsequently, it turned out that the $D0_{19}$ superstructure is a long-period close-packed one with lattice parameters a = 0.553 nm, b = 4.775 nm, and c = 0.432 nm [15, 17]. The latest studies confirmed that a long-period lattice is the most equilibrium lattice of this compound [18].

DEFORMATION OF AN Cu_3Sn LATTICE

Figure 2 shows a Cu_3Sn single-crystalline grain embedded in a thin-film Cu_6Sn_5 polycrystalline matrix. The grain has a prolate form 80 nm in height and 50 nm in width. Inside the grain, a large number of slip traces due to dislocation motion in the lattice are seen. Stresses causing the deformation of the Cu_3Sn grain are confined within the lattice of this grain, whereas neighboring Cu_6Sn_5 grains are free of dislocations. Moreover, an elastic-train-related contrast is not seen in the neighboring grains either. The deformation of a Cu_3Sn grain can be explained by superstructural compression because of crystal shrinkage due to ordering [19]. Such a stressed state of a grain can be characterized as uniform extension.

Thus, the given single-crystalline grain deforms by loading along a preferred axis, with the load being uniformly distributed over the grain. Such "equilibrium" loading allows the separation of preferred slip systems, determine dislocations, and find possible types of their reconfiguration early in plastic flow.

$D0_{19}$ alloys contain four main slip planes (Fig. 3): basal plane (0001), prismatic plane, and pyramidal I $\{\bar{1}100\}$ and pyramidal II $\{11\bar{2}1\}$ planes. Many electron microscopic studies [20–23], as well as theoretical calculations, demonstrate a strong dependence of slip along a given slip system on experimental conditions (temperature, strain rate).

Figure 4 shows the structure of the deformed Cu_3Sn single-crystalline grain. Crystallographic planes are distinctly seen, and somewhere diffraction conditions allow us to distinguish the atomic structure of the grain. In the top-left corner, a magnified image of the lattice's atomic structure with highlighted positions of atoms is shown. Direct measurements of the interatomic and interplanar distances suggest that this image is the projection onto the $(1\bar{1}00)$ crystallographic plane. Atomic rows in Fig. 4 consist of $\{11\bar{2}1\}$ planes, which are normal to the $(1\bar{1}00)$ one.

The electron micrograph in Fig. 4 shows that slip traces in the Cu_3Sn grain are parallel to $(\bar{1}\bar{1}21)$ and $(11\bar{2}1)$ planes. These planes belong to the pyramidal II slip system, which is a main slip system along with basal and prismatic slip systems. Figure 5 depicts the atomic structure of the $(1\bar{1}00)$ plane and shows the

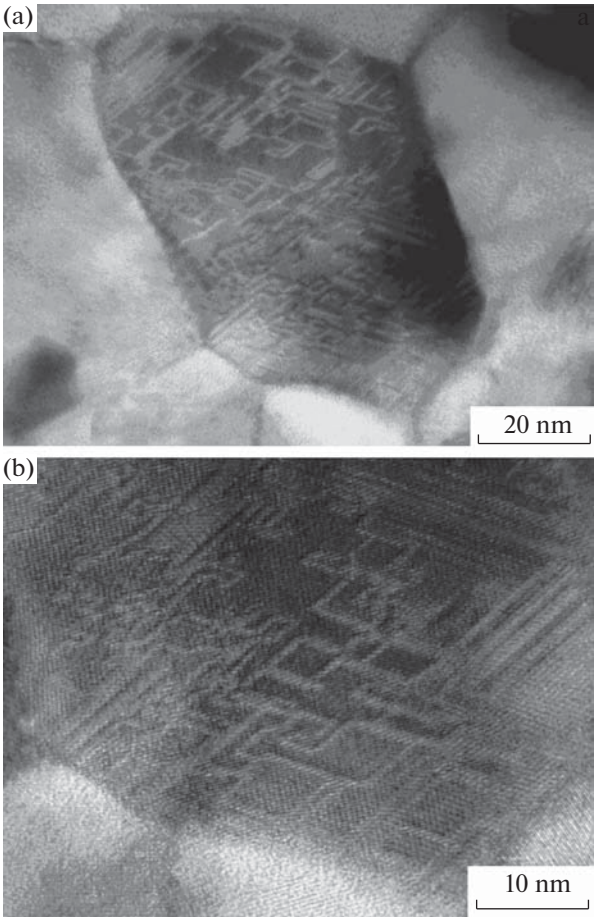

Fig. 2. (a) Deformed Cu_3Sn single-crystal grain surrounded by Cu_6Sn_5 grains and (b) magnified image of the crystal's bottom.

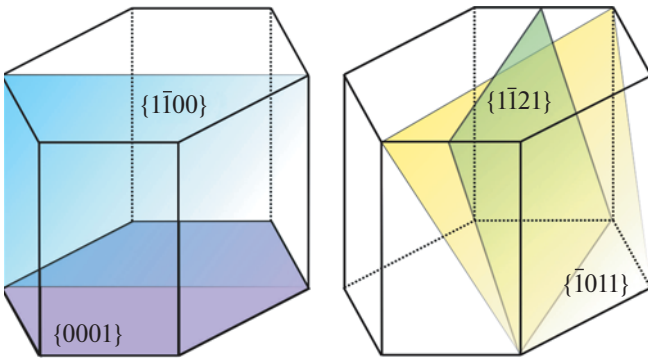

Fig. 3. Slip planes in $D0_{19}$ alloys.

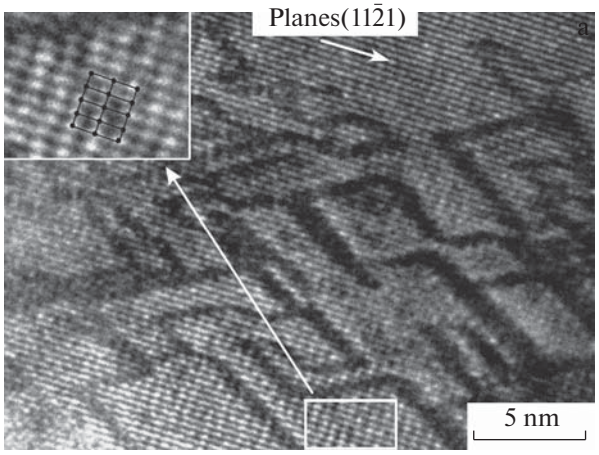

Fig. 4. Microstructure of the deformed Cu_3Sn single crystal under a high-resolution transmission electron microscope.

positions of projections of the (0001) basal plane and (11$\bar{2}$0) plane (which is normal to (0001)) relative to ($\bar{1}\bar{1}$21) and (11$\bar{2}$1) planes.

The edge dislocation shown in Fig. 6a represents an extra (11$\bar{2}$1) half-plane. Such dislocations are often encountered in the single-crystalline grain studied. However, the question as to whether their motion may lead to formation of observed slip systems remains unclear. Having analyzed the crystallographic slip in the slip trace, we came to the conclusion that the line of the trace is a stacking fault (SF) fringe. The typical slip trace and its highlighting (Figs. 6b, 6c) indicate that the amount of slip equals half the interplanar distance. Therefore, one can suppose that the trace is a result of motion of a complete, rather than a partial, dislocation. Considering that the crystal has a superstructure and slip is accomplished by a pair of superpartial dislocations, this defect may be categorized as a superstructural SF or a complex SF. In the latter case, it must also contain an antiphase boundary [26].

To speculate on the type of planar defect that arises behind a moving dislocation, it is necessary to find the slip direction. Since slip lines are parallel to {11$\bar{2}$1} planes, two slip directions are possible: ⟨2113⟩ and ⟨1126⟩. It is difficult to find which of these slip directions is activated by only observing slip line projections. It can be supposed that slip systems {1121}⟨1126⟩ are most likely in this case, since they were found in Ti_3Al deformed at temperatures below 573 K and in Ti_3Sn [12, 27]. In those studies, along with dislocations in the basal plane, widely dissociated dislocation pairs were observed on {1121} planes with a common Burgers vector of 1/3⟨1126⟩; however, dislocations with a Burgers vector of ⟨2113⟩ were absent. The core structure of dislocations lying in pyramidal I and pyramidal II planes in Ti_3Al was studied by computer simulation in [24, 25]. Simulation data showed that dislocations may slip over {1121} planes, splitting into superpartials with a Burgers vector of 1/6⟨1126⟩.

The most important result in [12] is that critical shear stress of slip in pyramidal slip system {1121}⟨1126⟩ is almost independent or even inversely

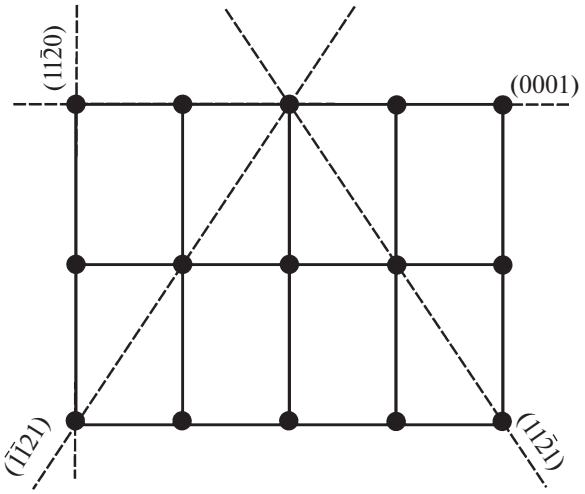

Fig. 5. (1 $\bar{1}$00) crystallographic plane.

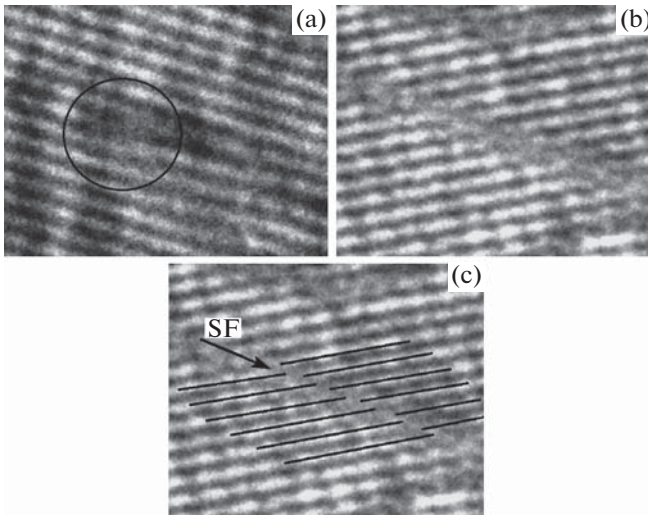

Fig. 6. (a) Dislocation, (b) crystallographic plane shift in a dislocation slip trace followed by SF formation, and (c) highlighting of crystallographic planes.

dependent on temperature. This may also indicate an anomalous temperature dependence of Cu_3Sn strength.

From Fig. 4 it follows that dislocation slip traces form a closed labyrinth configuration. In rare cases, the trace is broken with a dislocation at its end as a rule. All observed traces are oriented along {1121} planes. An interesting feature of slip traces is angular configurations, in which traces converge at an angle of 60° but do not intersect. Figure 7 shows angular configurations made up of slip traces and highlighted shift of crystal planes near angles. It was found that there is a dislocation near the vertex of the angle and that slip traces are SFs, which also end with dislocations.

One may assume that an angular configuration arises when a complete superdislocation splits into partials. For example, a superdislocation slipping in the basal plane may split into partials with a Burgers vector allowing slip in the pyramidal plane. In this case, a sessile configuration arises, which is associated with SF fringes. Theoretical analysis predicts a large number of pathways for the formation of such configurations.

CONCLUSIONS

Intermetallic Cu_3Sn is synthesized by condensing copper and tin on a substrate at 150°C. Cu_3Sn single crystals are notable for a developed labyrinth system of slip traces oriented along {1121} planes. Slip traces are the result of slipping in {1121}⟨1126⟩ slip systems. Cu_3Sn crystals, being ordered, exhibit a $D0_{19}$ superstructure. The amount of slip equals half the interplanar distance; that is, slipping in the $D0_{19}$ superstructure is accomplished by a pair of superstructural dislocations that form a superstructural SF. The deformation of Cu_3Sn crystals can be explained by superstructural compression because of crystal

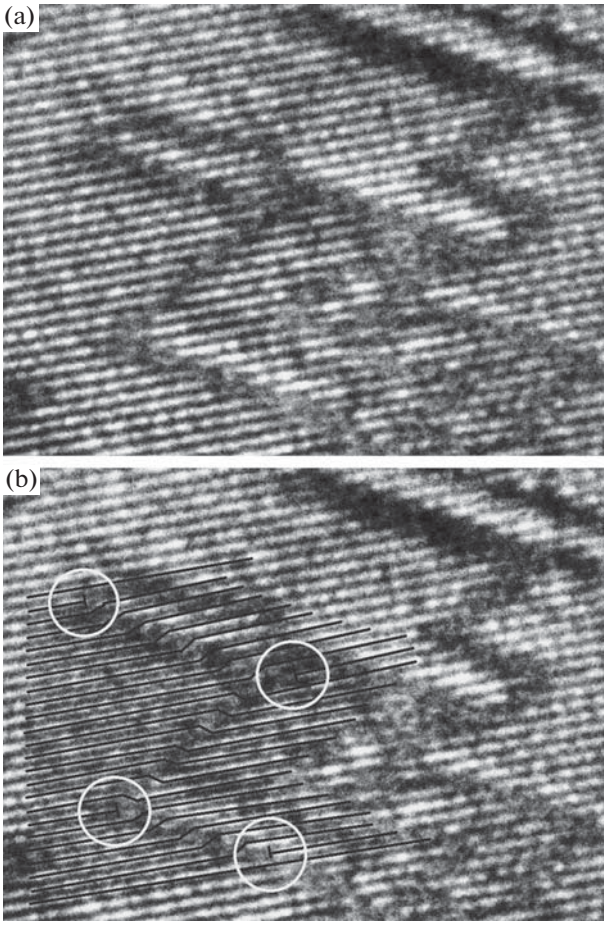

Fig. 7. Dislocation slip traces with the formation of angles and (b) highlighting of crystallographic planes and dislocations at the vertices of the angles.

shrinkage due to ordering. Such a stressed state of the crystal can be characterized as uniform extension.

REFERENCES

1. D. Yao and J. K. Shang, Metall. Mater. Trans. A **26**, 2677 (1995).
2. H. Flandorfer, U. Saeed, C. Luef, A. Sabbar, and H. Ipser, Thermochim. Acta **459**, 34 (2007).
3. S. W. Jeong, J. H. Kim, and H. M. Lee, J. Electron. Mater. **33**, 1530 (2004).
4. A. R. Fix, W. Nuchter, and J. Wilde, Soldering Surf. Mount Technol. **20**, 13 (2008).
5. T. Laurila, V. Vuorinen, and J. K. Kivilahti, Mater. Sci. Eng. R **49**, 1 (2005).
6. Y. Xia, X. Xie, and X. Xie, J. Mater. Sci. **41**, 2359 (2006).
7. B. Liu, Y. Tian, J. Feng, and C. Wang, J. Mater. Sci. **52**, 1943 (2017).
8. A. N. Makrushina and V. A. Plotnikov, in Proc. Int. Symp. "Advanced Materials and Technologies," Vitebsk, Belarus, 2017, p. 134.
9. D. H. Nam, R. H. Kim, D. W. Han, and H. S. Kwon, Electrochim. Acta **66**, 126 (2012).
10. M. Hansen and K. Anderko, *Constitution of Binary Alloys* (McGraw-Hill, 1965).
11. B. A. Grinberg and V. I. Syutkina, *New Methods for Strengthening Ordered Alloys* (Metallurgiya, Moscow, 1985).
12. T. Hashimoto, M. Nakamura, and S. Takeuchi, Mater. Trans. **31**, 195 (1990).
13. J. D. Bernal, Nature **122**, 54 (1928).
14. W.-H. Chen, C.-F. Yu, H.-C. Cheng, and S.-T. Lu, Microelectron. Reliab. **52**, 1699 (2012).
15. Y. Watanabe, Y. Fujinaga, and H. Iwasaki, Acta Crystallogr. B **39**, 306 (1983).
16. P. L. Brooks and E. Gillam, Acta Metall. **18**, 1181 (1970).
17. C. J. Muller and S. Lidin, Acta Crystallogr. B **70**, 879 (2014).
18. S. Furtauer, D. Li, D. Cupid, and H. Flandorfer, Intermetallics **34**, 142 (2013).
19. A. A. Klopotov, A. I. Potekaev, E. V. Kozlov, Yu. I. Tyurin, K. P. Aref'ev, N. O. Solonitsina, and V. D. Klopotov, *Crystallogeometrical and Crystallochemical Laws of Formation of Binary and Ternary Compounds Based on Titanium and Nickel* (Tomsk. Politekh. Univ., Tomsk, 2011).
20. Y. Minonishi and M. H. Yoo, Philos. Mag. Lett. **61**, 203 (1990).
21. Y. Minonishi, Philos. Mag. A **63**, 1085 (1991).
22. Y. Umakoshi, T. Nakano, T. Takenaka, K. Sumimoto, and T. Yamane, Acta Metall. Mater. **41**, 1149 (1993).
23. M. Legros, A. Couret, and D. Caillard, Philos. Mag. A **73**, 81 (1996).
24. L. I. Yakovenkova, L. E. Karkina, and M. Ya. Rabovskaya, Tech. Phys. **48**, 1280 (2003).
25. R. Oguma and S. Matsumura, Trans. Mater. Res. Soc. Jpn. **40**, 325 (2015).
26. M. D. Starostenkov and B. F. Dem'yanov, Metallofiz. Noveishie Tekhnol. **7**, 128 (1985).
27. S. A. Court, J. P. A. Lofvander, M. H. Loretto, and H. L. Fraser, Philos. Mag. A **59**, 379 (1989).
28. L. I. Yakovenkova, L. E. Karkina, and M. Ya. Rabovskaya, Tech. Phys. **48**, 56 (2003).

Translated by V. Isaakyan

SPELL OK